Fast-track 'coloured' inversion

*Steve Lancaster * BP Amoco, Sunbury UK*
David Whitcombe BP Amoco, Aberdeen UK

Summary

Inversion of seismic data to Acoustic Impedance is usually seen as a specialist activity, so despite the publicised benefits, inverted data are only used in a minority of cases. To help overcome this obstacle we aimed to develop a new algorithm which would not necessarily be best in class, but would be quick and easy to use and increase the use of inversion products within BPA. This new technique, 'Coloured Inversion', performs significantly better than traditional fast-track routes such as recursive inversion, and benchmarks well against unconstrained sparse-spike inversion.

Empirical study has revealed that unconstrained sparse-spike inversion can be approximately modeled as a convolutional process, with an operator whose amplitude spectrum maps the mean seismic spectrum to the mean earth AI spectrum, and has a phase of -90^o. In addition, following reflectivity work by Walden & Hosken (1985) we have found that the gross spectral form of AI logs from wells in any given field is reasonably constant. This implies that a single convolutional operator can be used to perform inversion. The approach assumes a zero-phase wavelet but does not need an explicit estimate of the wavelet amplitude spectrum. The zero-phase assumption can be compensated for by phase rotation of the inverted data in comparison with the AI logs.

Once the Coloured Inversion operator has been derived it can be simply applied to the data on the interpretation workstation as a 'user-defined filter'. In this way inversion can be achieved within hours since the volume data do not have to be exported to another package, and no explicit wavelet is required.

Introduction

With the advent of multi-version interpretation of AVO and 4D, many 3D volumes now need inverting. Current fast-track methods for band-limited inversion to relative impedance are usually direct unconstrained transforms of the seismic data, such as phase rotation, trace integration and recursive inversion, and as such are prone to error because no account is taken of the seismic wavelet or calibration made to the earth. More sophisticated techniques such as sparse-spike inversion do take account of these factors, but require specialist skills to implement correctly. The technique described here implicitly accounts for the seismic wavelet, is consistent with log data, yet is easy and fast to implement. Additionally it benchmarks well against unconstrained Sparse-Spike inversion. With Coloured Inversion (CI) we are now able to routinely invert any dataset within hours and establish a base-case against which all subsequently more sophisticated techniques must be judged.

Method

In Figure 1, zero-phase data from the North Sea have been inverted using an unconstrained Sparse-Spike algorithm.

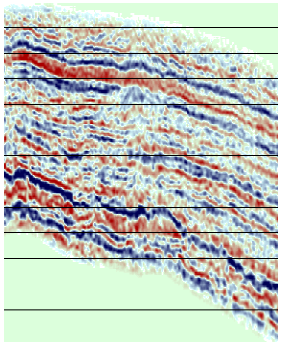

Figure 1: North Sea data inverted using a sparse-spike algorithm

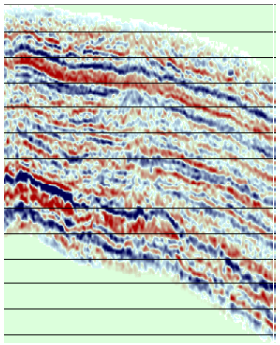

Figure 2: Result of cross-matching input seismic to the data in Figure 1

By cross-matching these impedance data with the input reflection data we derive a single optimal matching filter (Figure 3). Convolving this filter with the input data we see in Figure 2 that the result is very similar to the inverted data, everywhere. This empirical observation indicates that inversion can be approximated with a simple filter, and that it may be valid over a sizeable region.

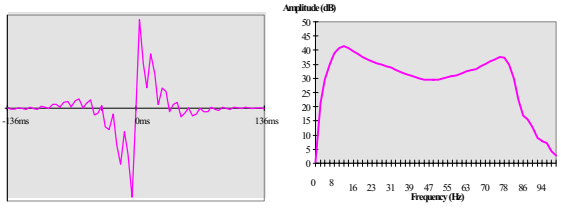

Figure 3: Matching operator that optimally converts input seismic to sparse-spike inversion. Convolving this with the seismic gives the data in Figure 2.

So is it possible to derive this operator without knowing the answer first ? The phase of the operator is a constant -90° which is in agreement with the simplistic view of inversion being akin to integration, and the concept of a zero-phase reflection spike being transformed to a step AI interface, provided the data are zero-phase. But what about the operator's amplitude spectrum ?

Walden & Hosken's (1984) empirical observation tells us that all earth reflection coefficient series have spectra that exhibit a similar trend that can be simply described as f^{β}. The β term is a positive constant and f is frequency. Velzeboer (1981) arrives at a similar observation theoretically. β may vary from one field to another but tends to remain reasonably constant within any one field. We have observed similar behaviour for AI spectra, but now the exponent is negative, and to distinguish it from the reflection series exponent we refer to it here as α.

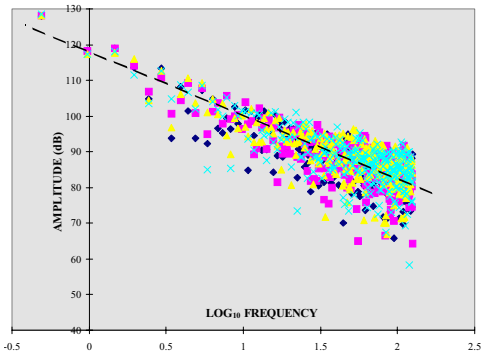

Figure 4: Four AI logs from a North Sea field are displayed on a log-frequency axis to demonstrate the linear trend, equivalently exponential on a linear frequency axis. The gradient of the linear fit determines α.

It follows therefore that if our seismic data are inverted correctly they too should show the same spectral trend as logs in the same area, i.e. have the same value of α. If we find α for a field by curve-fitting to AI logs then the amplitude spectrum of the inversion operator is determined as being that which maps the mean seismic spectrum to a curve of form f^{α}. All that is needed to derive our CI operator are AI logs over the zone of interest and enough seismic traces to form a good estimate of the mean seismic response. Once the CI operator has been derived it can easily be applied using standard interpretation software, thus avoiding having to export whole 3D volumes to an external inversion package, then re-import the result.

The seismic wavelet amplitude spectrum does not need to be determined since it dictates the shape of the mean input seismic spectrum, which is automatically compensated for through the CI operator. If the phase of the wavelet is not zero or is unknown, then this will be manifested as a phase error in the inversion, as phase rotation and convolution are commutative processes. The phase can usually be approximated as linear over the inversion bandwidth and so can be determined by phase rotating the inversion and comparing with AI logs. This phase correction can then be applied post-inversion on the interpretation workstation.

Figure 5 shows a comparison between the matching operator (also shown in Figure 3) and the Coloured Inversion operator derived for these data using the procedure outlined. Clearly these two operators are very similar and so we have succeeded in deriving a practical inversion operator.

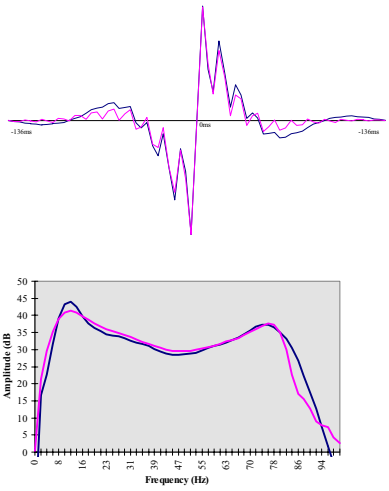

Figure 5: Comparison of the matching operator (pink) and the Coloured Inversion operator (dark blue).

Real Data Example

For the field used in Figure 1 above, AI logs from 22 wells were examined. For each log spectrum α was estimated by least-squares curve-fitting and the results displayed as in Figure 6. A general consistency between the wells can be observed, and a representative α for the whole field chosen, taking into account the reliability of individual logs based on active length and logging quality.

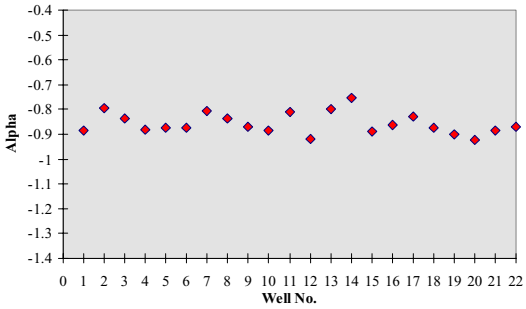

Figure 6: Results of fitting a curve of the form f^{α} to each of 22 wells from the same North Sea field. A value of -0.85 was chosen to represent the whole field in this case.

Using this value of α, a Coloured Inversion operator was constructed, once a mean seismic spectrum had been obtained. Figure 7 shows a comparison of the Sparse-spike inversion from Fig. 2 and the Coloured Inversion result. The two inversions are very similar, but the Coloured Inversion took far less time and effort to achieve.

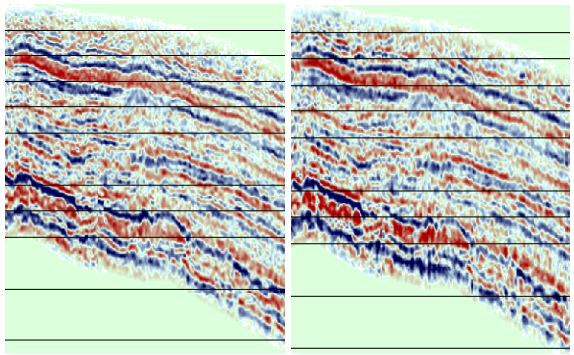

Figure 7: North Sea data inverted using a sparse-spike algorithm (left) and Coloured Inversion (Right)

Synthetic Example

A 2D full-bandwidth AI model was constructed using real well logs and interpreted horizons from another North Sea field. This was then converted to reflection coefficients and convolved with a typical wavelet for the area at a target depth of approximately 3.0s. By applying a zero-phase band-pass filter to the full-bandwidth AI data a section was obtained against which inversion schemes could be benchmarked (Figure 8). In this example no noise was added to the synthetic data.

Here we show the comparative results between unconstrained sparse-spike and Coloured Inversion.

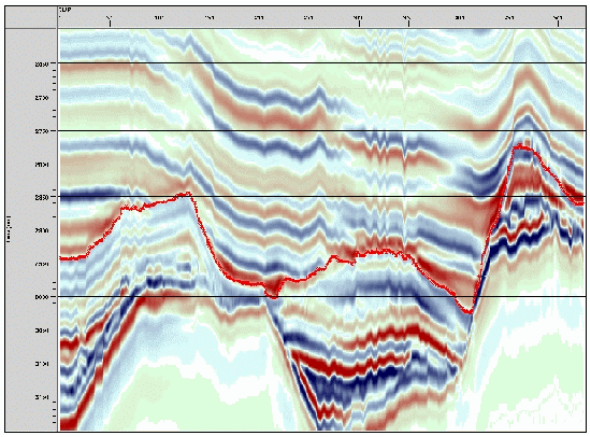

Figure 8: Benchmark dataset - 'the answer'

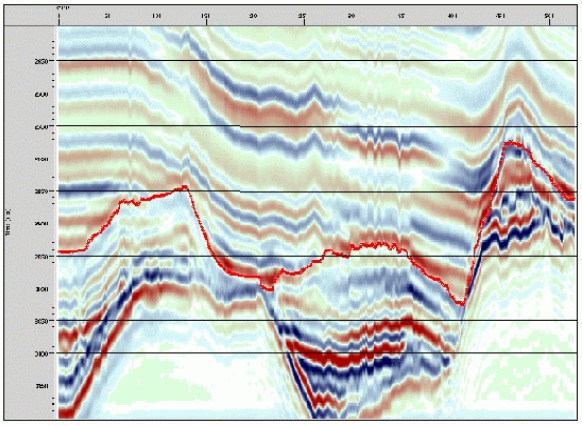

Figure 9 : Unconstrained Sparse-Spike Inversion

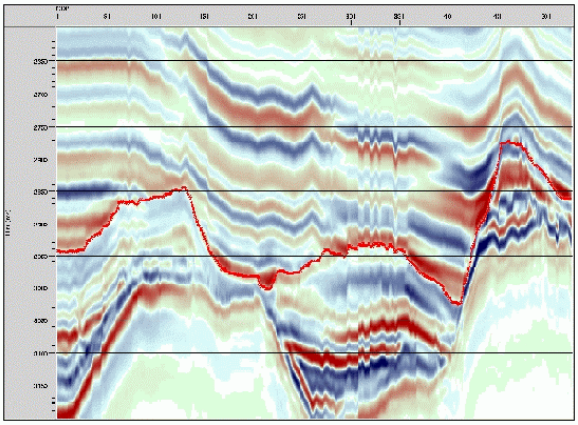

Figure 10 : Coloured Inversion

As with the real data example above the initial impression is that the two inversion schemes produce very similar results. The red horizon is displayed on each, and shows that gross timing of events is the same for each version. On closer examination however differences become apparent.

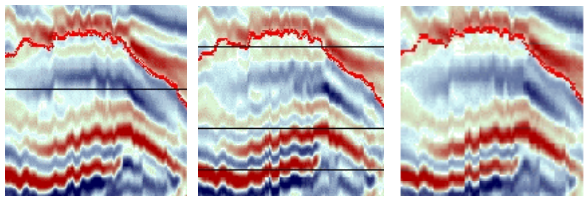

Figure 11 : Synthetic inversion study, close comparison of results.

From Figure 11 we see that Sparse-spike inversion seems to have achieved better resolution than either the Coloured Inversion or the Benchmark ! After some investigation looking closely at the parameterization of the sparse-spike inversion it became apparent that the reason for this difference was due to small errors in the wavelet estimation (Figure 12). Despite being noise-free synthetic data, the wavelet estimation method of matching seismic to well - reflectivity is not perfect. Small errors in this single wavelet can manifest themselves as consistent errors in the inversion, and so can be mis-interpreted as geological detail. From Figure 12 it is clear that the dominant frequencies in the wavelet have been predicted correctly, but that errors exist in the low and high frequency detail of the tails. In the synthetic displays shown here we see evidence of the high frequency error; a low frequency error would be manifested as striping if the data were not low-cut filtered.

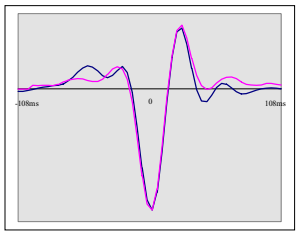

Figure 12 : Wavelet comparison, actual (black) v estimated (pink).

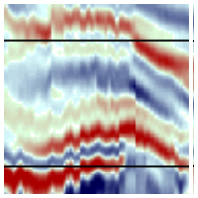

Figure 13 : sparse-spike using correct wavelet

As a check, the sparse-spike inversion was re-run using the actual wavelet used in constructing the synthetic data, and this time a closer tie to the benchmark was achieved.

Conclusions

Coloured Inversion enables the rapid inversion of 3D data. A single convolutional inversion operator is derived that optimally inverts the data and honours available well data in a global sense. In this way the process is inherently stable and broadly consistent with known AI behaviour in the area. Construction of the operator is a simple process and implementation can be readily performed on most interpretation workstations. No explicit wavelet is required other than testing for a residual constant phase rotation as the last step. This removes an inherently weak-link that more sophisticated processes rely on.

Since only a single convolution is applied, the process is a direct transform of the seismic data, which implies that the result can be viewed as a base-case, showing what information in the AI domain comes directly from the seismic. Use of subsequent inversion methods, that employ constraints and/or a-priori models, can be compared with the Coloured Inversion to determine what the additional constraints have contributed to our image of the AI domain, over and above that from the seismic.

Coloured Inversion assumes that adequate noise attenuation has been performed, so that the seismic spectrum within the frequency bounds defined for the inversion is dominated by the contributions from the seismic wavelet and earth reflectivity. However, the process can be iterated so that further noise attenuation is performed on an initial inversion, and a correction filter applied to re-shape the spectrum to the measured earth spectrum.

References

Walden, A.T., and Hosken, J.W.J., 1985. An investigation of the spectral properties of primary reflection coefficients. Geophysical Prospecting , 33, 400-435

Velzeboer, C.J., 1981. The theoretical seismic reflection response of sedimentary sequences. Geophysics Vol. 46, No. 6, pp843-853

Acknowledgements

The authors would like to thank the BP Amoco board for permission to publish this material, and to Michael Bush, Keith Nunn, Sue Raikes and Terry Redshaw for their valuable contributions to the development of concept and code.